CALCULATION OF MODE PARAMETERS OF WALL BEAD DEPOSITION IN DOWNHAND MULTI-PASS GAS-SHIELDED WELDING

M.A. SHOLOKHOV and **D.S. BUZORINA**
«Shtorm» Ltd.
28 Bazhov Str., Verkhnyaya Pyshma, RF. E-mail: ekb@shtorm-its.ru

Application of narrowed grooves is an effective method to increase welding process efficiency at simultaneous reduction of financial and energy expenses. One of the main difficulties in implementation of multi-pass welding technology 10 mm thick rolled metal structures using automated and robotized units is a high possibility of defect formation such as lack of penetration, in particular, in layer of the first pass (wall bead). Control of welding parameters determining heat input is one of the methods of penetration regulation. Dependencies between welding parameters in problem areas of the grooves and penetration depth were determined experimentally. On their basis the equations for determination of parameters of bead deposition at given coefficient of areas were obtained. These results became a part of algorithm development to control welding mode parameters in automated and robotized units. 12 Ref., 1 Table, 6 Figures.

Keywords: *mechanized consumable electrode welding, total heat efficiency of welding process, full-factor experiment, coefficient of areas, mathematic modelling, determination of parameters of welding mode*

Increase of welding process efficiency is still a relevant problem under conditions of current welding production. Application of narrowed grooves [1] is one of the proficient methods allowing significantly increasing welding process efficiency as well as reducing financial and energy expenses. Along with it the efficiency increase requires implementation of automatic and robotized systems. However, in realization of multi-pass consumable electrode welding technology on automatic and robotized units some difficulties appear, related to defect formation such as lack of penetration. In particular in wall bead deposition [2], in order to obtain the weld metal with needed mechanical properties, favorable structure, minimal deformation and required weld shape, as well as lower possibility of hot and cold cracks formation [3] it is necessary decreasing heat input. Under conditions of decreased heat input in multi-pass welding due to increased heat abstraction to base metal the possibility of lack of fusion between bead and groove edges, as well as the nearby beads, considerably grows.

One of the regulation methods of the base metal penetration in groove problem areas is changing of process parameters (current, voltage, speed of welding), that determine heat input and, therefore, weld formation conditions, in particular, depth of edge penetration [4, 5].

Work [6] covers the study results of welding mode parameters influence (reversed polarity welding current, arc voltage, distance between electrode tip and edge) on wall bead shape in submerged arc welding. It was determined that the parameter, which defines mechanical jamming of slag crust, is an angle of transfer of wall bead surface to the edge. The main parameters of mode determining its value are the arc voltage, distance between electrode tip and edge as well as welding speed. However, this study does not cover the questions of preparation angle influence on lack of penetration near bevel edge.

There is also a well-known method, when to prevent the lack of penetration between bead and bevel edge, the automatic welding with weaving and increased pulsed current towards edge being welded is used. However, determination of accurate value of pulse power is necessary for that (due to evaluation of efficiency use of arc heat energy).

Thus, issues regarding determination of bevel angle influence on bead formation, optimization of groove parameters, as well as modes of setting of wall bead deposition with given area coefficient k equal ratio of penetration area to deposition area F_{pen}/F_d, which guarantees absence of lack of penetration, are still relevant.

The aim of the present work is the determination of dependencies between parameters of wall bead deposition in mechanized multi-pass gas-shielded welding and penetration depth, as well as definition of modes of wall bead deposition with set area coefficient based on obtained dependencies.

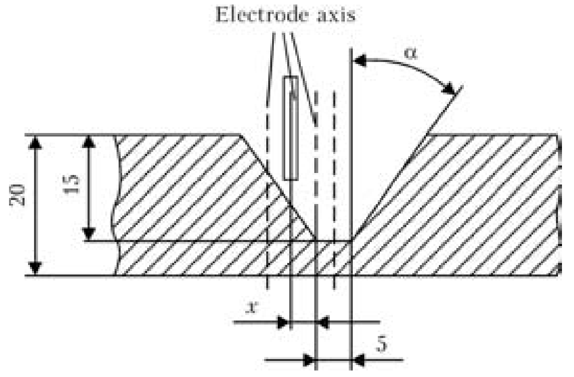

Figure 1. Scheme of bead passing

Efficient control of penetration of metal being welded under conditions of arc welding is possible only having information about main dependencies of this process, as well as qualitative and quantitative effect of welding mode parameters on size and shape of penetration zone. Statistically recognized dependencies between energy parameters of welding mode (welding current, arc voltage, welding speed etc.), on the one hand, and parameters, characterizing quality of welded joint, on the other hand, make a basis of the most mathematical models developed for welding process control. Depth of penetration of welded metal and area of weld section [7, 8] refer to the parameters determining weld geometry and quality of welded joint. Efficiency of application of arc heat energy for formation of welded joint is evaluated using total heat efficiency of welding process η_w, which determines the ratio of conditional heat input of weld metal being fused per time unit to heat power of welding heat source [5]:

$$\eta_w = \frac{v_w F_{weld} \gamma_m H_{melt}}{Q} = \frac{v_w (F_{weld} + F_{pen}) \gamma_m H_{melt}}{Q} = \eta_d + \eta_{pen}, \quad (1)$$

where v_w is the welding speed, m/s; F_{weld} is the area of weld cross section, m^2; F_d is the area of deposited metal section, m^2; F_{pen} is the area of penetration of base metal, m^2; γ_m is the specific density of metal, kg/m^3, which equals 7850 kg/m^3 for low-carbon steel; H_{melt} is the enthalpy at melting temperature taking into account open melting heat, J/kg, H_{melt} = 1340 J/g [5] is taken for low-carbon steel; $Q = IU$ is the heat power of welding heat source, J/s; η_d, η_{pen} is the total heat efficiency of process of deposition and penetration of base metal [9].

Procedure of experiment. Present paper studies the effect of technological parameters (bevel angle α, position of electrode in bevel — distance between electrode tip and edge — coordinate x, as well as welding speed v_w) on bead section area and total heat efficiency of process in mechanized gas-shielded welding for evaluation of dependence of wall bead formation on geometry of bevel and position of electrode in terms of formation of high quality wall bead.

Welding was carried out by bead passing in accordance with scheme, given in Figure 1. Samples from 09G2S steel (0.5–0.8 Si, 1.3–1.7 Mn, 0.30 Cu, 0.30 Ni, 0.040 S, 0.12 C, 0.035 P, 0.30 Cr, 0.008 N, 0.08 As) that are 200 × 500 × × 20 mm plates simulating welded joint with 15, 25, 35° grooving and shoulder 5 mm similar to performed root pass were used. System for experimental studies (Figure 2) includes table with current supply, autocarriage Noboruder NB-5H and welding machine S5 Pulse SHTORM-LORCH. Parameters of welding mode were registered with the help of devices installed on the control panel of welding machine.

SG2 welding wire 1.2 mm diameter (analog Sv-08G2S according to GOST 2246–70) and mixed shielding gases 82 % Ar and 18 % CO_2 according to TU 2114-004-00204760–99 were used for welding.

Values of factors were changed in accordance with plan of full-factor experiment (Table).

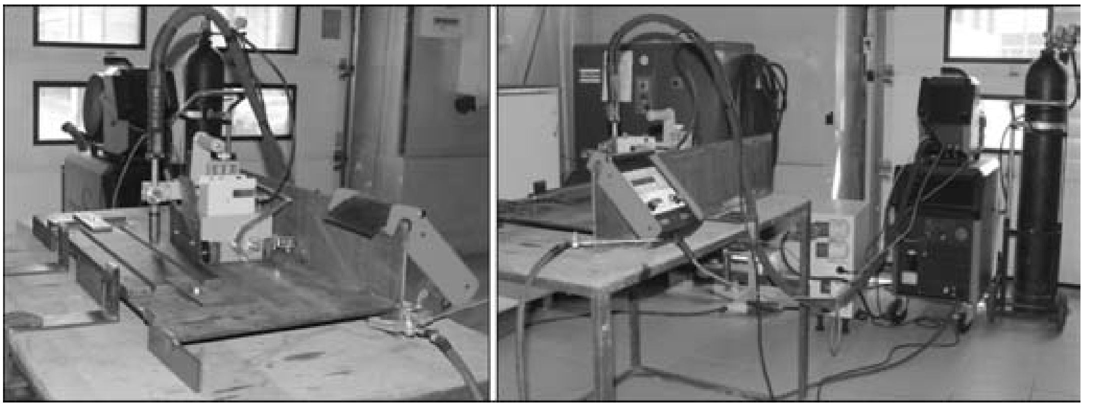

Figure 2. General view of welding installation

Factor	Value		
	−1	0	+1
Bevel angel α, deg (x_1)	15	25	35
Distance from axis to electrode x, mm (x_2)	0	1.5/2/4	2.5/4/7
Welding speed, m/h (x_3)	18	24	30

Welding mode was selected so as to provide satisfactory weld formation:

welding current I_w, A .... 217 ± 10
wire feed rate $v_{w.f}$, m/min 6.3
arc voltage U_a, V .... 214 ± 1
consumption of shielding gas, l/min 18
electrode diameter d, mm 1.2
electrode stickout, mm .... 20 ± 1

Using measurement of manufactured macrosections (Figure 3) of welded joints, bead section area was determined, and total heat efficiency coefficient was calculated on formula 1.

On the basis of experimental data, regressive equation was obtained:

$$F_V(\alpha, x, v_w) = 47.498 - 0.031\alpha + 4.205x - 0.956v_w - 0.113\alpha x + 0.003\alpha v_w - 0.143xv_w + 0.004\alpha x v_w \ (\mathrm{mm}^2), \quad (2)$$

as well as total neat efficiency of welding process:

$$\eta_V(\alpha, x, v_w) = 0.1253 - 0.0055\alpha + 0.018x + 0.0239v_w + 0.00006\alpha^2 + 0.0006x^2 - 0.0005v_w^2 - 0.0005\alpha x + 0.00012\alpha v_w - 0.00013xv_w. \quad (3)$$

Analysis of results and their generalization. Analysis of obtained dependencies of bead section area and total heat efficiency on welding speed showed that they have complex nature during electrode movement within groove width. Namely under the same conditions (v_w, α) during electrode movement to the edge the values of bead section area and efficiency increase, and under other conditions they decrease. Such dependence might be explained by mutual influence of groove geometry and parameters of welding mode, that characterize electrode (arc) position towards the molten metal interlayer. With increase of welding speed, bead section area reduces and total heat efficiency of welding process increases only to specific value. This might be explained by the fact that with increase of welding speed, quantity of metal being deposited per unit of weld length reduces [9]. However, at that, arc column starts to deviate sideway opposite to the welding direction with the increase of welding speed. Deviating arc column displaces part of liquid metal in tail part of the pool. Thinning of liquid interlayer under the arc provides the increase of penetration depth at rise of welding speed up to specific value. Depth of penetration decreases at further speed increase due to reduction of heat input.

Given results match well with data of papers [10, 11] from which we know that the speed of movement in liquid increases as it leaks to the bottom of crater and thickness of film at first rises, and then reduces. Thickness of film and, in particular, speed of metal movement in it significantly depend on parameters of welding (deposition) mode.

Besides, it is known that [12] distribution of specific power of heat flow over the surface of groove and weld pool has complex nature due to interaction of the arc with surface of the weld pool. Distribution of heat flow also significantly changes at alteration of welding mode due to change of form of the weld pool surface, as well as positioning of electrode in the grooves. Therefore, the most broad picture of heat influence of the arc in gap welding can be determined only using simulation of weld pool formation and ex-

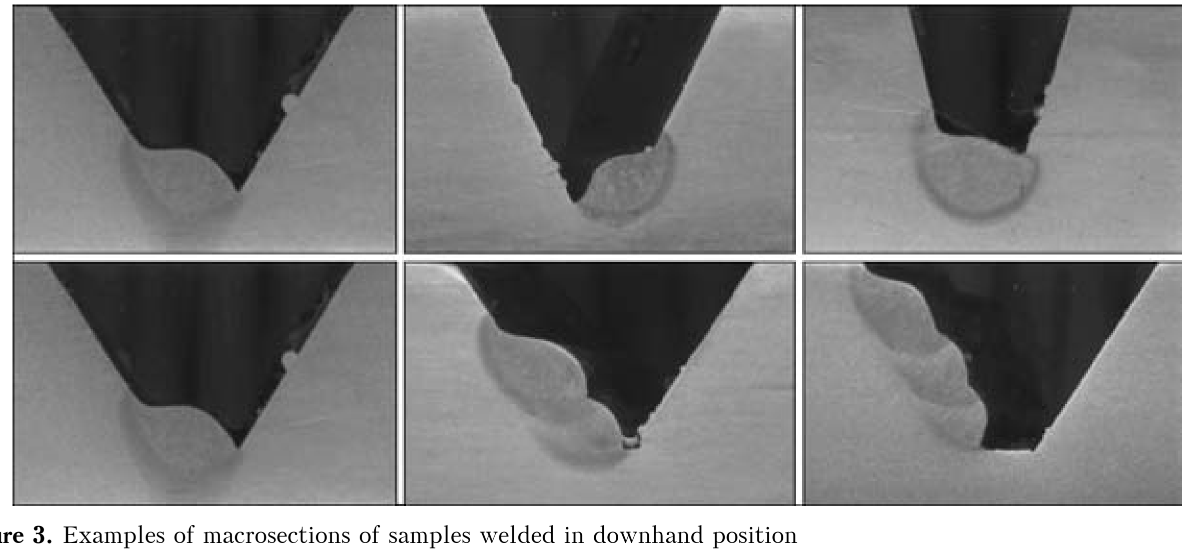

Figure 3. Examples of macrosections of samples welded in downhand position

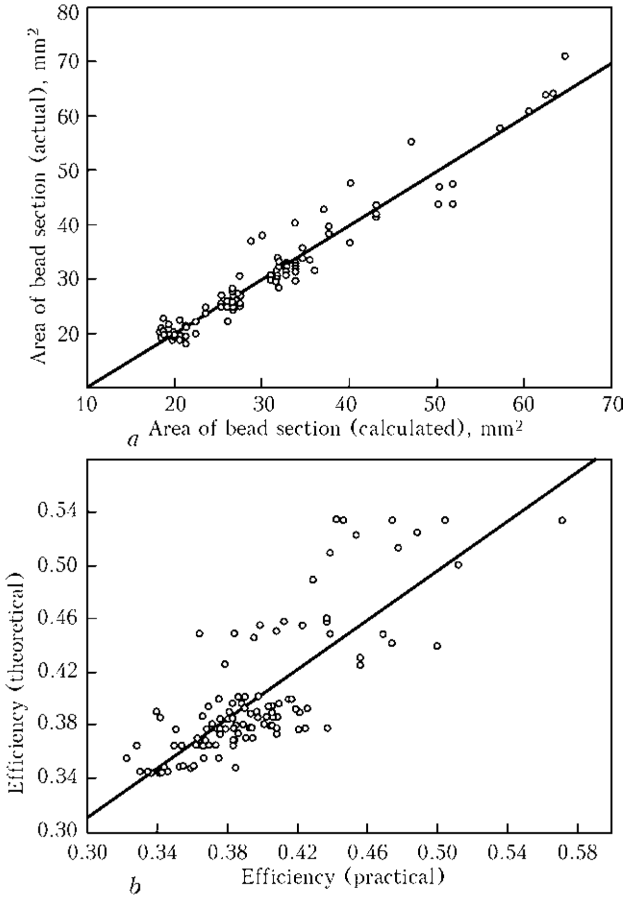

Figure 4. Diagram of scattering of experimental (*circles*) and calculated (*solid line*) values of area of bead section (*a*) and heat efficiency (*b*) of welding process

perimental studies taking into account the groove shape and specific welding mode.

Obvious conclusion about combined influence of parameters of welding mode and liquid interlayer under the arc on weld formation can be made based on the mentioned above. Therefore, it should be considered in the equations used for determination of bead section area and heat efficiency. In this case, they are represented in multiplicative form and written in the following way:

$$F = F_V(\alpha, x, v_w)\theta_F(I_w), \quad (4)$$

$$\eta_w = \eta_V(\alpha, x, v_w)\theta_\eta(I_w), \quad (5)$$

where $F_V(\alpha, x, v_w)$, $\eta_V(\alpha, x, v_w)$ are the functions of dependence of area of bead section and heat effect on bevel angle α, electrode position in groove x, speed of welding v_w; $\theta_F(I_w)$, $\theta_\eta(I_w)$ are the functions of dependence of area of bead section and heat efficiency on welding current I_w, respectively.

Functions $\theta_F(I_w)$, $\theta_\eta(I_w)$ were determined in a course of experiment:

$$\theta_F(I_w) = 0.0134 I_w - 1.559, \quad (6)$$

$$\theta_\eta(I_w) = 0.0047 I_w + 0.084. \quad (7)$$

Conformity of obtained equations (4) and (5) were evaluated using diagrams of scattering of experimental and calculated values of bead section area and heat efficiency of the welding process (Figure 4).

Diagrams of scattering, given in Figure 4, show satisfactory matching of theoretical and experimental values of bead section area and heat efficiency of the welding process. Conformity control of obtained equations using Fisher F-criterion gave positive results that characterize their accuracy.

Problem (as inverse) on determination of modes of welding with set bead section area and coefficient of areas k was solved based on experimental and theoretical data. Given dependencies were determined and obtained in the following form:

- welding current

$$I_w = \frac{-b + \sqrt{b^2 - 4ac}}{2a}; \quad (8)$$

coefficients a, b, c are determined using following formulae:

$$a = -0.015\frac{\pi d^2}{F_d}; \quad b = 0.637 + \frac{\pi d^2}{F_d}(3.341 - 0.01\alpha);$$

$$c = -74.048 + 0.048\alpha - \frac{\pi d^2}{F_d}(185.97 - 0.583\alpha) - (1 + k_f)F_d,$$

where k_f is the coefficient of fusion in consumable electrode welding, it equals 0.18–4 at applied modes;

- voltage

$$U_{ef} = \frac{B_{ef} v_{w.f}}{\eta_w I_w}; \quad (9)$$

coefficient B_{ef} is determined on formula

$$B_{ef} = \gamma_m H_{melt}\frac{1 + k_f}{4}\pi d^2;$$

- welding speed

$$v_w = \frac{\pi d^2(0.08 I_w - 8.32)\cdot 60}{4F_d} \text{ (m/h)}. \quad (10)$$

Experiments for verification of convergence of obtained dependencies in this study and of evaluation convergence of results of welding parameters determination using obtained equations (8)–(10) were carried out, and graphs of welding current values convergence (Figure 5) and diagram of scattering of actual and calculated voltage values (Figure 6) were built on their basis.

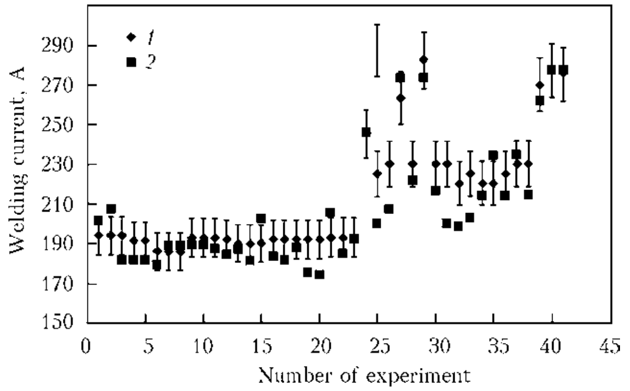

Figure 5. Diagram of convergence of experimental (*1*) and calculated (*2*) values of welding current (error ±5 %)

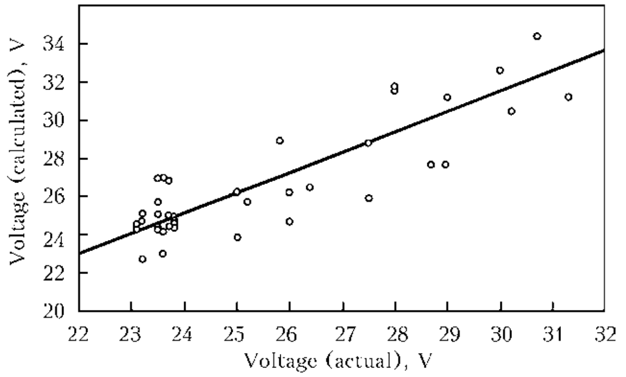

Figure 6. Diagram of scattering of experimental (*circles*) and calculated (*solid line*) values of voltage

As can be seen from Figures 5 and 6 , scattering of values does not exceed 10–12 %, therefore, these equations for determination of parameters of mode of wall bead deposition (also can be used for calculation of parameters of mode of deposition on inclined surface) can be used in development of technology of mechanized multi-pass shielded-gas welding.

Conclusions

1. General equations of dependence of welding process heat efficiency and bead section area on technological parameters of welding were formulated and obtained in analytical form. The equations (except for known parameters) take into account mutual effect of electrode position relatively to liquid metal pool ($F_V(\alpha, x, v_w)$, $\eta_V(\alpha, x, v_w)$) and value of interlayer of molten metal under the arc ($\theta_F(I_w)$ and $\theta_\eta(I_w)$).

2. Obtained equations allow calculating parameters of deposition of first bead in the layer, which provide for set coefficient of areas $k = F_{pen}/F_d$ (in considered limits of k from 0.20 up to 1.57), and as a result reduction of possibility of appearance of such defects as lack of penetration.

3. Optimum values of bevel angle $\alpha = 20.3°$ and speed of welding $v_w = 26.34$ m/h were determined for given parameters of mode with the help of obtained equations under condition of maximum value of total heat efficiency of welding process $\eta_w = 0.392$. The most efficient heat input is provided at given values of bevel angel and speed of welding.

4. Program for calculation of wall bead deposition modes was developed based on results of performed work.

5. Obtained analytical dependencies can be used in the future for development of algorithms to control of welding mode parameters in automatic and robotized units.

1. Rakhmatullin, T.A., Sholokhov, M.A., Buzorina, D.S. (2012) Problems of implementation of narrowed gaps in welding of hull structures of special engineering. *Izvestiya Vuzov. Mashinostroenie*, **4**, 64–66.
2. Berezovsky, B.M. (2003) *Mathematical models of arc welding*. Vol. 2: Mathematical modeling and optimization of formation of different type welds. Chelyabinsk: YuUrGU.
3. Goncharov, N.S. (2009) *Investigations and development of technology of twin-arc shielded-gas automatic welding of hulls from high strength medium alloy steels*: Syn. of Thesis for Cand. of Techn. Sci. Degree. Ekaterinburg.
4. Lebedev, V.A. (2011) Control of penetration in mechanized welding and surfacing. *Svarochn. Proizvodstvo*, **1**, 3–11.
5. Erokhin, A.A. (1973) *Basics of fusion welding. Physical-chemical principles*. Moscow: Mashinostroenie.
6. Chernyshov, G.G., Pankov, V.V., Markushevich, I.S. (1984) Influence of mode parameters on formation of wall bead in welding with deep grooves. *Svarochn. Proizvodstvo*, **12**, 14–16.
7. Berezovsky, B.M. (2002) *Mathematical models of arc welding*. Vol. 1: Mathematical modeling and information technologies, models of weld pools and weld formation. Chelyabinsk: YuUrGU.
8. Sas, A.V., Gladkov, E.A. (1983) Technological process of welding as a object in ACS. *Izvestiya Vuzov. Mashinostroenie*, **8**, 144–146.
9. (2007) *Theory of welding processes*: Manual. Ed. by V.M. Nerovny. Moscow: N.E. Bauman MGTU.
10. Razmyshlyaev, A.D. (1982) Hydrodynamic parameters of liquid metal film on the front wall of pool crater in arc welding. *Avtomatich. Svarka*, **1**, 20–25.
11. Potapievsky, A.G. (1974) *Consumable-electrode shielded-gas welding*. Moscow: Mashinostroenie.
12. Sholokhov, M.A., Oskin, I.E., Erofeev, V.A. et al. (2012) Distribution of arc heat power in consumable-electrode narrow-gap welding. *Svarka i Diagnostika*, **4**, 18–23.

Received 03.06.2013